FGFR1 Emerges as a Potential Therapeutic Target for Lobular Breast Carcinomas

Jorge Sergio Reis-Filho,[1,2] Pete T. Simpson,[3] Nicholas C. Turner,[1] Maryou Ballo Lambros,[1] Chris Jones,[4] Alan Mackay,[1] Anita Grigoriadis,[1] David Sarrio,[6] Kay Savage,[1] Tim Dexter,[1] Marjan Iravani,[1] Kerry Fenwick,[1] Barbara Weber,[5] David Hardisson,[7] Fernando Carlos Schmitt,[2] Jose Palacios,[6] Sunil R. Lakhani,[3] and Alan Ashworth[1]

Abstract

Purpose: Classic lobular carcinomas (CLC) account for 10% to 15% of all breast cancers. At the genetic level, CLCs show recurrent physical loss of chromosome16q coupled with the lack of E-cadherin (*CDH1* gene) expression. However, little is known about the putative therapeutic targets for these tumors. The aim of this study was to characterize CLCs at the molecular genetic level and identify putative therapeutic targets.

Experimental Design: We subjected 13 cases of CLC to a comprehensive molecular analysis including immunohistochemistry for E-cadherin, estrogen and progesterone receptors, HER2/neu and p53; high-resolution comparative genomic hybridization (HR-CGH); microarray-based CGH (aCGH); and fluorescent and chromogenic *in situ* hybridization for *CCND1* and *FGFR1*.

Results: All cases lacked the expression of E-cadherin, p53, and HER2, and all but one case was positive for estrogen receptors. HR-CGH revealed recurrent gains on 1q and losses on 16q (both, 85%). aCGH showed a good agreement with but higher resolution and sensitivity than HR-CGH. Recurrent, high level gains at 11q13 (*CCND1*) and 8p12-p11.2 were identified in seven and six cases, respectively, and were validated with *in situ* hybridization. Examination of aCGH and the gene expression profile data of the cell lines, MDA-MB-134 and ZR-75-1, which harbor distinct gains of 8p12-p11.2, identified *FGFR1* as a putative amplicon driver of 8p12-p11.2 amplification in MDA-MB-134. Inhibition of *FGFR1* expression using small interfering RNA or a small-molecule chemical inhibitor showed that *FGFR1* signaling contributes to the survival of MDA-MB-134 cells.

Conclusions: Our findings suggest that receptor *FGFR1* inhibitors may be useful as therapeutics in a subset of CLCs.

Grade 1 invasive ductal breast carcinomas and classic lobular carcinomas (CLC) are remarkably similar at the molecular genetic level. Like grade 1 invasive ductal breast carcinoma, CLC show deletions on chromosome 16q, but the genes affected by the deletion are different (1–4). Although the 16q target gene of grade 1 invasive ductal breast carcinoma remains elusive (4), there are several lines of evidence to suggest that *CDH1*, which maps to 16q22.1 and encodes the transmembrane intercellular adhesion glycoprotein, E-cadherin, is the target gene in CLCs (5–7). Loss of E-cadherin is a common feature of several types of malignancies (4–8), and may explain some of the hallmark features of CLC, i.e., the discohesiveness of the cells and the typical single cell file invasion pattern, as well as the peculiar proclivity of metastatic spread to serosal cavities (5–7).

Although several mechanisms of *CDH1* gene inactivation and E-cadherin down-regulation have been reported in lobular carcinomas, including *CDH1* gene promoter methylation, *CDH1* gene mutations, loss of heterozygosity (LOH) on 16q22, and deletion (physical loss) of 16q (1, 2, 5–7, 9–13), little is known about the pathogenic role of other genetic alterations in this special type of breast cancer. Amplification and/or overexpression of HER2 (14, 15) and epidermal growth factor receptor are rare in CLCs (15). There is evidence to suggest that cyclin D1 (*CCND1*) gene amplification and overexpression is frequently found in CLCs (16, 17). Moreover, the involvement of tumor suppressor genes other than *CDH1* in the biology of CLCs has not been evaluated in detail.

Currently, the mainstay of treatment for CLCs is with adjuvant endocrine therapy as they are usually positive for

Authors' Affiliations: [1]The Breakthrough Breast Cancer Research Centre, Institute of Cancer Research, London, United Kingdom; [2]IPATIMUP-Institute of Molecular Pathology and Immunology, University of Porto, Porto, Portugal; [3]Molecular and Cellular Pathology, Mayne Medical School, University of Queensland, Queensland Institute of Medical Research and Royal Brisbane and Women's Hospital, Brisbane, Australia; [4]Section of Paediatric Oncology, Institute of Cancer Research, Sutton, United Kingdom; [5]University of Pennsylvania, Philadelphia, Pennsylvania; and [6]Centro Nacional de Investigaciones Oncológicas, and [7]Department of Pathology, La Paz Hospital, Madrid, Spain

Received 5/15/06; revised 8/14/06; accepted 8/28/06.

The costs of publication of this article were defrayed in part by the payment of page charges. This article must therefore be hereby marked *advertisement* in accordance with 18 U.S.C. Section 1734 solely to indicate this fact.

Note: Supplementary data for this article are available at Clinical Cancer Research Online (http://clincancerres.aacrjournals.org/).

J.S. Reis-Filho, P.T. Simpson, and N. Turner contributed equally to the present study.

Requests for reprints: Jorge S. Reis-Filho, The Breakthrough Breast Cancer Research Centre, Institute of Cancer Research, Fulham Road, London SW3 6JB, United Kingdom. Fax: 44-207-153-533; E-mail: jorgerf@icr.ac.uk.

doi:10.1158/1078-0432.CCR-06-1164

estrogen receptors. However, they continue to pose a therapeutic challenge due to the lower than expected response rates to endocrine therapy (18) and neoadjuvant chemotherapy (19, 20). Hence, there is a pressing need for more therapeutic options in this disease. In this study, we subjected a well-characterized series of CLCs to a comprehensive genetic analysis with the aims of characterizing their molecular genetic features and identifying potential novel therapeutic targets in this subtype of breast cancer.

Materials and Methods

Tumor samples

Eighteen paraffin-embedded cases of infiltrating lobular carcinoma were retrieved from the Department of Pathology, La Paz Hospital, Madrid, Spain. Paired normal tissue samples (unaffected lymph nodes or normal breast tissue) were available for all tumors. The study had approval from the local ethics committees.

Immunohistochemistry

Sections from representative areas were cut at 4 μm and mounted on silane-coated slides. Immunohistochemistry was done according to the streptavidin-biotin-peroxidase complex method as previously described (6, 21), with antibodies raised against E-cadherin (4A2C7, 1:200, Zymed, San Francisco, CA), β-catenin (C19220, 1:1000; Transduction Labs, Lexington, KY), estrogen receptor (1D5, 1:40; Dako, Glostrup, Denmark), progesterone receptor (PgR636, 1:150; Dako), HER2 (polyclonal, 1:1200; Dako), p53 (DO7, 1:150; Dako), cyclin D1 (CCND1, SP4, 1:50, LabVision, Fremont, CA), and fibroblast growth factor receptor 1 (FGFR1, polyclonal, 1:600; Abcam, Cambridge, United Kingdom).

Positive and negative controls were included in each slide run. For estrogen receptors, progesterone receptors, p53, and CCND1, only nuclear staining was considered positive, whereas only membranous staining was considered specific for Her2/neu, E-cadherin, and FGFR1. A cutoff of ≥10% of positive neoplastic cells was adopted for estrogen receptors, progesterone receptors, p53, CCND1, and FGFR1; Her2/neu was analyzed according to the Herceptest scoring system, and E-cadherin and β-catenin were semiquantitatively analyzed as previously described (6); briefly, the intensity (compared with normal luminal epithelial cells) and the extent of immunoreactive cells was determined. Cases were considered negative for E-cadherin or β-catenin when strong membrane staining was observed in <5% of tumor cells; as "reduced" when the staining intensity was clearly weaker than that observed in normal luminal epithelial cells or when <20% are positively stained; and as "conserved" when >50% of cells showed positive staining with an intensity equal to that of normal luminal epithelial cells (6).

DNA extraction

DNA was isolated from needle microdissected whole tumor sections followed by phenol/chloroform extraction and ethanol precipitation as previously described (6, 21). Normal DNA was obtained from paired normal tissue when available.

Molecular analysis

Microarray-based comparative genomic hybridization. The microarray-based comparative genomic hybridization (aCGH) platform used in this study was constructed by the Breakthrough Breast Cancer Research Centre, UK and comprised one platform comprised of ~5,600 BAC clones spaced at ~0.9 Mb throughout the genome. BAC clones were spotted in triplicate onto Corning GAPSII-coated glass slides (Corning, NY). Labeling, hybridization, and washes were carried out as previously described (21). Arrays were scanned with a GenePix 4000A scanner; fluorescence data were processed with GenePix 4.1 image analysis software (Axon Instruments, Inc., Union City, CA).

Data analysis

The $\log_2$ ratios were normalized for spatial and intensity-dependent biases using a group row local regression. The median of BAC clone replicate spots was calculated, after exclusion of excessively flagged clones (flagged in >70% of samples). The median $\log_2$ ratio for each clone in each "dye-swap" was rescaled according to the local median absolute deviation, and averaged across the replicates (dye-swaps). In the study of CLCs and breast cancer cell lines, this left a final data set of 4,816 clones and 3,527 clones with unambiguous mapping information according to the May 2004 build of the human genome (hg17), respectively. Data were smoothed using a local polynomial adaptive weights smoothing procedure for regression problems with additive errors. A categorical analysis was applied to the BACs after classifying them as representing gain, loss, or no-change according to their smoothed $\log_2$ ratio values. For the CLCs, median absolute deviation–centered $\log_2$ ratio values less than −0.8 were categorized as losses, those >0.8 as gains, and those in between as unchanged, whereas for the normalized cell line data, the cutoff described by Reis-Filho et al. (21) was used. Data preprocessing (normalization, filtering, and rescaling) was done using S Plus (version 6.2.1, Insightful Corporation, Seattle, WA). Data statistical analysis was carried out in R 2.0.1 (http://www.r-project.org/) and BioConductor 1.5 (http://www.bioconductor.org/), making extensive use of modified versions of the packages, in particular aCGH, marray, and adaptive weights smoothing (21).

Associations between genomic loci were assessed by a calculating a Euclidean distance metric between thresholded values for each clone, assigned as 1, 0, or −1 for gain, no change, or loss in copy number. Only those clones with a DNA copy number change in at least 2 out of 13 samples were plotted. Positive associations (small Euclidean distance) are shown in orange, negative associations (large Euclidean distance) are shown in purple. White represents no association or no (<2 out of 13 cases) alterations. Hierarchical clustering was done on categorical data (i.e., gain, no change, and loss) based on a Euclidean distance measure using Ward's minimum variance method.

High-resolution CGH

Amplification and fluorescent labeling of DNA from microdissected tissue was carried out by degenerate oligonucleotide-primed PCR in two rounds and CGH was done as previously described (21).

cDNA microarrays

Total RNA was isolated from breast cancer cell lines using TriZol LS reagent (Invitrogen, Carlsbad, CA) followed by phenol/chloroform extraction. RNA quality was verified using an Agilent Bioanalyzer (Agilent Technologies, Palo Alto, CA). Total RNA was T7-amplified and labeled using the amino allyl MessageAmp kit (Ambion, Huntingdon, United Kingdom) according to the manufacturer's instructions. Five micrograms of amino-allyl aRNA was cohybridized with universal human reference RNA (Stratagene, La Jolla, CA) to a cDNA microarray constructed at The Breakthrough Breast Cancer Research Centre, containing ~20,000 sequence-validated cDNA clones, corresponding to ~16,500 known genes. Dye swap duplicates with both Cy3 and Cy5 labeled targets were hybridized separately in 50% formamide and 1× microarray hybridization buffer (Amersham) at 42°C for 18 hours under lifter slips. Following hybridization, arrays were washed twice in 2× SSC, 0.1% SDS for 15 minutes at 42°C, and twice in 0.1× SSC, 0.1% SDS for 15 minutes at 42°C. Following a brief rinse in 0.1× SSC, arrays were dried and scanned on GenePix 4000 (Axon Instruments) dual-color confocal laser scanner and raw intensity measurements were obtained through GenePix software 5.1.

After removing flagged and low-intensity microarray features, data was printTipLoess normalized using the limma package in R 2.0.1 (http://www.r-project.org/). A total of 16,593 clones were mapped according to the May 2004 build of the human genome (hg17). Mapped cDNA clones and BACs were overlaid using a plotting script written in R 2.0.1 (making use of modified versions of aCGH, marray, and limma packages). Heat maps were generated using Java TreeView software.

Fluorescent and chromogenic *in situ* hybridization

Fluorescent *in situ* hybridization (FISH) and chromogenic *in situ* hybridization were used to allow a direct evaluation of the copy number changes in nonneoplastic and invasive lobular carcinoma cells. The probes used included the ready-to-use digoxigenin-labeled SpotLight cyclin D1 amplification probe (Zymed) and an in-house generated probe made up of three contiguous, FISH-mapped BACs (RP11-350N15, RP11-148D21, and RP11-359P11; ref. 22), which map to 8p12-p11.23 (~38.26 and ~38.6 Mb). The in-house probe was generated, biotin-labeled, and used in hybridizations as previously described (22). Chromogenic *in situ* hybridization experiments were analyzed by two of the authors (J.S. Reis-Filho and K. Savage) on a multiheaded microscope. For FISH experiments, representative images were collected sequentially in three channels (4′,6-diamidino-2-phenylindole, FITC, and Cy3) on a TCS SP2 confocal microscope (Leica, Milton Keynes, United Kingdom). Only unequivocal signals were counted. Signals were evaluated at ×400 (chromogenic *in situ* hybridization) and ×1,000 (FISH), and 60 morphologically unequivocal neoplastic cells were counted for the presence of the gene probe signals. Amplification was defined as more than five signals per nucleus in >50% of cancer cells, or when large gene copy clusters were seen (22). All *in situ* hybridization were evaluated with observers blinded to the aCGH result.

Molecular characterization of the *CDH1* gene

Detailed analysis of the *CDH1* gene has been described elsewhere (15). Briefly, the complete *CDH1* gene was screened for mutations using single-strand conformational polymorphism–PCR DNA sequencing (15). LOH analysis in tumor and paired normal DNA was carried out using five highly polymorphic microsatellite markers (D16S265, D16S3057, D16S398, D16S496, and D16S752, which map to 16q21.2-q22) and the frequent CDH1 + 2076C/T polymorphism (15). To avoid the underestimation of LOH due to normal cell contamination in the tumor samples, DNA from the infiltrating areas was extracted by LCM using a PixCell laser capture microscope (Arcturus Engineering, Mountain View, CA). *CDH1* gene promoter hypermethylation was assessed by methylation-specific PCR of bisulfite-treated DNA (6).

Cell lines and reagents

MDA-MB-134, ZR-75-1, CAL51, and MCF7 cell lines (American Type Culture Collection, Manassas, VA) were maintained in DMEM (Sigma, Poole, United Kingdom) supplemented with 10% v/v fetal bovine serum, glutamine, and antibiotics. *FGFR1* small interfering RNA (siRNA) SMARTpool reagent (M-003131-02), and nontargeting control siRNA 1 (D-001210-01) were obtained from Dharmacon (Chicago, IL). *FGFR1* tyrosine kinase inhibitor SU5402 (ref. 23; Calbiochem, San Diego, CA) was dissolved in DMSO.

RNAi transfection and survival assays

Cells were plated 24 hours before transfection in 96-well plates. Cells were transfected with predesigned siRNA (Dharmacon) at a final concentration of 100 nmol/L using Oligofectamine (Invitrogen) as per the manufacturer's instructions. Five days following transfection, cell survival was assessed using CellTitre-Glo Luminescent cell viability assay (Promega, Madison, WI). To assess the sensitivity to the FGFR1 tyrosine kinase inhibitor, SU5402 (23), cells were plated in 96-well plates and 24 hours after plating exposed to various doses of SU5402. Medium containing drugs were replaced after 48 hours, and cell survival was assessed using CellTitre-Glo Luminescent Cell Viability Assay after 5 days.

Western blotting

Lysates from transfected cell pellets were made 72 hours following transfection, in 50 mmol/L Tris (pH 8.0), 150 mmol/L NaCl, 0.5% sodium deoxycholate, 1% NP40, 0.1% SDS, and protease inhibitors. Lysates were electrophoresed using Novex 4%-12% Bis-Tris precast gels (Invitrogen) and immunoblotted with anti-FGFR1 ab10646 (Abcam) or anti-α-tubulin T9026 (used as a loading control; Sigma), followed by anti-IgG horseradish peroxidase and chemiluminescent detection.

Results

Immunohistochemical characterization of CLCs

We examined 13 cases of CLC that were selected for optimal CGH and aCGH hybridization from 18 previously described cases (6). The immunohistochemical phenotype of these tumors is characteristic of CLC (Table 1). Briefly, 12 cases were positive for estrogen receptors and 6 of these were also positive for progesterone receptors. No p53 nuclear expression was identified. No cases showed overexpression of HER2. Twelve cases completely lacked E-cadherin expression, whereas one

Table 1. Summary of the immunohistochemical and molecular findings in 13 cases of CLC

Case	Grade	Estrogen receptor	Progesterone receptor	p53	HER-2	E-Cadherin	β-Catenin	*CDH1* mutations	*CDH1* methylation	LOH 16q21-22	Loss 16q (HR-CGH)	Loss 16q22.1 (aCGH)
LC18	2	+	+	–	0	–	–	Wild-type	UN	LOH	Loss	Loss
LC22	2	+	–	–	0	–	–	Ex12, codon613	UN	LOH	Loss	Loss
LC32	2	+	+	–	0	–	–	Wild-type	UN	No LOH	Loss	No
LC33	2	+	–	–	0	–	–	Wild-type	UN	LOH	Loss	Loss
LC38	2	–	–	–	0	–	–	Wild-type	MET	LOH	Loss	Loss
LC40	2	+	+	–	0	–	–	Wild-type	UN	LOH	Loss	Loss
LC50	2	+	–	–	0	–	–	Wild-type	MET	No LOH	Loss	Loss
LC51	2	+	–	–	0	–	–	Wild-type	MET	LOH	Loss	Loss
LC57	2	+	+	–	0	–	–	Ex7, codon288	MET/UN	LOH	Loss	Loss
LC58	2	+	+	–	0	–	–	Wild-type	MET/UN	No LOH	Loss	Loss
LC62	2	+	+	–	0	–	–	Wild-type	UN	N.I.	Loss	Loss
LC71	2	+	–	–	1+	–/+	–	Wild-type	UN	N.I.	No	Loss
LC73	2	+	+	–	0	–	–	Wild-type	MET/UN	LOH	Loss	Loss

NOTE: –, lack of expression; –/+, reduced expression; +, positive; Grade, Scarff-Bloom-Richardson grade.

showed significantly reduced membrane staining. All cases lacked β-catenin membrane staining.

aCGH confirms the genetic complexity of CLCs

The frequency of DNA copy number alterations for each clone in our sample set is shown in Fig. 1A. As described by Shelley-Hwang et al. (13) and Loo et al. (12), a significant proportion of the genome showed alterations: a median of 1,178 BACs [range, LC58 (742)-LC57 (3,531) BACs], representing 24.46% of the genome, showed either gains or losses of genetic material. Gains were more frequent than losses, affecting a median of 791 BACs (12.39% of the genome) and 597 BACs (16.42% of the genome), respectively. Overall, the most common copy number changes observed in >30% of the samples were gains of chromosomes 1q, 5p, 7q, 11p, 11q, 12q, 14q, 16p, 18p, 19p+q, and 20p+q, and losses on chromosomes 11q, 13q, 16q, 18q, and Xq (Supplementary Table S1). aCGH analysis confirmed the presence of recurrent regions reported to be gained or lost in low-grade ductal and lobular breast carcinomas (i.e., 1q+, 11q−, and 16q−). Given that DNA amplification methods were not used in the cases analyzed by aCGH, and that aCGH provides more accurate profiles for pericentromeric and telomeric regions than CGH (2, 12, 13), chromosomes 16p, 19p, and 22 could be reliably analyzed in the present study.

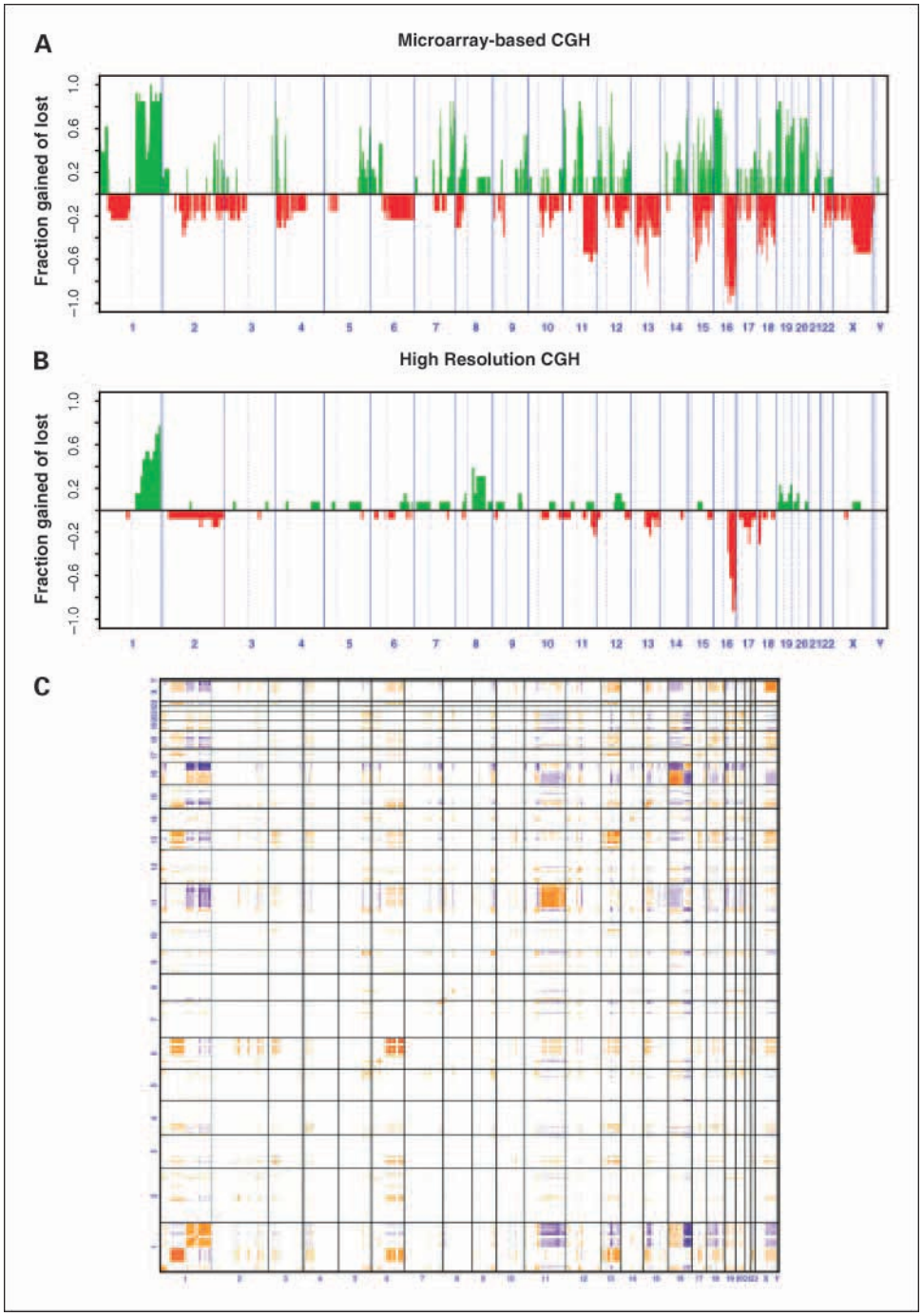

Fig. 1. Frequency of copy number changes in CLCs. Overall frequency of DNA copy number alterations found in 13 CLCs as defined by aCGH (*A*) and HR-CGH (*B*). *A,* individual BAC clones are plotted according to genomic location along the *X*-axis. The proportion of tumors in which each clone is gained (*green bars*) or lost (*red bars*) is plotted along the *Y*-axis. Vertical dotted lines, chromosome centromeres. *B,* cytogenetic bands are plotted according to their genomic location along the *X*-axis. The proportion of tumors in which each cytogenetic band is gained (*green bars*) or lost (*red bars*) is plotted along the *Y*-axis. Vertical dotted lines, chromosome centromeres. *C,* association matrix of copy number changes based on Euclidean distance. The heat map shows positive associations (small Euclidean distance; *orange*) and negative associations (large Euclidean distance; *purple*).

Gains and losses of whole chromosomes or chromosomal arms were reliably detected by aCGH. However, the increased resolution of aCGH also allowed the identification of the most frequently altered regions within these large-scale gains and losses. For instance, the minimal region of gains on 11q mapped to the cytogenetic bands 11q12-q13.4, which encompasses several candidate oncogenes such as cyclin D1 (*CCND1*), fibroblast growth factor 19 (*FGF19*), fibroblast growth factor 4 (*FGF4*), fibroblast growth factor 3 (*FGF3*), and myeloma overexpressed gene (*MYEOV*).

Figure 1B and Supplementary Table S1 summarize the recurrent gains and losses observed in ≥30% of the cases. Gains affecting small regions (<15 Mb) were identified in genomic loci harboring genes which have been reported to be amplified and/or overexpressed in human carcinomas (Table 2). For instance, focal gain of genomic material was identified on 3q27.1 (in 46% of cases), which encompasses two transcription factors: the translation initiation factor 4G (*EIF4G-1*) and ets variant gene 5 (*ETV5*). A small gain on chromosome 2q37.1, encoding the *WNT6* gene, was observed in 30.8% of the cases. Gain of 5p15.33, the genomic locus of telomerase reverse transcriptase (*h-TERT*), was seen in 61% of cases. Gains on 12q were observed in 12 (92%) cases, with the minimal region of amplification mapping to 12q13.2-12q14.1, which encompasses multiple gene candidates, including cyclin-dependent kinase 2 (*CDK2*), cyclin-dependent kinase 4 (*CDK4*), sarcoma-amplified sequence (*SAS*), glioma-associated antigen (*GLI1*), centaurin-γ1 (*CENTG1*), and *C-ERBB3* (*HER3*). Table 2 summarizes genes mapping to small regions (≤20 Mb) of recurrent losses observed in >30% of the samples. Interestingly, copy number polymorphisms have been described in these regions (refs. 24, 25; http://projects.tcag.ca/variation/). Although increased copy number of genes mapping to these regions may play a role in the biology of lobular cancers, we cannot determine whether these copy number gains represent germ line copy number polymorphisms conferring an elevated susceptibility to lobular carcinomas or are tumor-specific changes. Further studies are required to clarify this issue.

Validation of aCGH

High-resolution CGH. To validate the results of aCGH, all cases were subjected to high-resolution CGH (HR-CGH). Genomic alterations were identified in all cases. The number of chromosomal arms with aberrations ranged from 3 to 15 per case (median, six changes / case). The number of gains ranged from one to nine gains / case (median, three gains / case) and losses ranged from one to seven (median, four losses / case; Fig. 1B; Supplementary Table S2). The most frequent recurrent gains comprised 1q (11 cases), 8q (6 cases), and 8p and 19p (both, 3 cases), whereas the most frequent recurrent losses were 16q (12 cases), and 11q, 13q, 17q, and 18 p (all, 4 cases). Concurrent gain of 1q and loss of 16q, regarded as a hallmark feature of low grade ductal carcinomas and lobular carcinomas, were seen in 12 of 13 cases (76.9%). The agreement between chromosomal arm changes detected by aCGH and HR-CGH ranged from 47% to 100% (median, 88%; mean, 80%), with aCGH showing a markedly increased resolution and sensitivity (Fig. 1; Supplementary Fig. S1).

Fluorescent and chromogenic* in situ *hybridization. To further validate specific gains of genomic material identified by aCGH, *in situ* hybridization was done in two sets of samples: five cases with gains of 8p12-p11.2 and five cases with gains of 11q13. The results were confirmed in all cases (Fig. 2). In these experiments, adjacent stromal cells (fibroblasts, lymphocytes, and macrophages) and residual normal breast lobules and ducts were used as internal controls, and showed normal copy numbers, ruling out possible copy number polymorphisms.

E-cadherin is down-regulated in CLCs by a combination of genetic and epigenetic mechanisms

By aCGH, deletion (physical loss) of 16q22.1 was observed in all cases, 12 of them including the genomic locus of the *CDH1* gene (16q22.1-67.3 Mb, see below). A number of different mechanisms of *CDH1* gene silencing were observed (Table 1). In two cases, *CDH1* gene was silenced by a combination of physical loss and *CDH1* frameshift truncating mutations (6). In five cases, *CDH1* gene was inactivated by a combination of physical loss and *CDH1* gene promoter methylation. Out of the remaining six cases, physical loss of 16q22.1 was detected in five cases. In one case (LC32), a partial deletion of 16q was detected by HR-CGH, however, the telomeric boundary of the deleted region could not be well defined. Interestingly, no LOH on 16q21-q22 or deletion on 16q22.1, as defined by aCGH, was found. This case exemplifies the greater accuracy of aCGH in mapping regions harboring deletions (12, 13, 21). The use of aCGH and LOH proved invaluable to detect losses on 16q22.1: two cases that were not informative by LOH showed loss of 16q22.1. In addition, aCGH and chromosomal HR-CGH revealed loss of 16q22.1 in two out of three cases that showed no LOH at this region. As previously described, aCGH seemed to be more sensitive than chromosomal HR-CGH for detecting loss of genomic material in the presence of normal cell contaminants (21). For instance, in case LC71, aCGH revealed loss of 16q22.1, whereas LOH analysis was not informative and chromosomal CGH showed only a trend for loss of 16q.

CLCs frequently harbor complex genetic aberrations on 8p

The short arm of chromosome 8 showed an intriguing pattern of genomic changes. Loss of 8p was seen in four cases, including one with loss of the whole arm, and three cases harboring partial deletions of 8p. The minimal deleted region encompassed 8p23.3-8p22, the genomic location of several putative tumor suppressor genes, including deleted in liver cancer-1 (*DLC-1*), which is reported to be deleted in up to 40% of all breast carcinomas, GATA-binding protein 4 (*GATA4*), and tumor suppressor candidate 3 (*N33/TUSC3*; ref. 26). In these cases, the deleted regions were followed by high-level gains of 8p12-p11.23, suggesting that the "break-fusion-bridge" may be the underlying genetic mechanism for this amplicon (26–28). Interestingly, gains of 11q13 followed by losses of 11q14.1-qter were also found in these samples (Fig. 2). Gains of 8p were detected in three additional cases, and in these six cases, the minimal region of genomic gain spanned 2 Mb (36.9-38.9 Mb). This amplicon encompasses multiple genes reported to play roles in breast cancer progression (16, 28–37), such as fibroblast growth factor receptor 1 (*FGFR1*; refs. 16, 28, 31–35), transforming acidic coiled coil gene 1 (*TACC1*; ref. 36), and eukaryotic translation initiation factor 4E-binding protein 1 (*EIF4EBP1*; ref. 37; Table 2).

Table 2. Small recurrent gains (<15 Mb) and losses (<20 Mb) of genomic material in >30% of the samples

Cytogenetic bands	Start (kb)	End (kb)	Putative oncogene
Gains			
2q33.1-q33.3	199,000	205,000	*DPP4, FZD7*
2q33.3-q34	207,000	210,000	*CREB1, FZD5*
2q35	216,000	222,000	*WNT6,WNT10A, PTPRN, DSP*
2q37.1	232,000	234,000	*EIF4E2*
3q27.1-q27.3	184,000	187,000	*EIF4G1, ETV5, EPHB3, ABCC5, MAP3K13*
4p16.3-p15.33	248	11,276.68	*FGFR3, SNURF, RNF4, GAK, TACC3*
4p14	39,260	41,111.01	*HIP2, UCHL1*
5p15.33	368	1,869.006	*TERT*
5q31.2-q32	136,000	144,000	*FGF1,CDC25, EGR-1*
5q33.1-q33.2	148,000	154,000	*CDX1, PDGFRB, GPX3*
5q34-q35.3	168,000	181,000	*FGF18, FGFR4, FOX1, ETEA, STK10, RAB24, VEGFR-3, SRC2*
6p21.33-p12.3	31,367	46,265.01	*TNF, VEGF*
7q11.23-q21.11	71,713	77,318.47	*FZD9, CLDN4, CLDN3, PTPN12*
7q22.1	96,873	103,000	*ZFP95, SERPINE1,CLDN15*
8p12-p11.21	33,711	423,48.47	*SPFH2, BRF2, RAB11FIP1, FLJ14299, PROSC, EIF4BP1, ASH2L, LSM1, BAG4, DDHD2, HTPAP, WHSC1L1, AP3M2, IKBKB, FGFR1, EIF4EBP1, TACC1, C8ORF4, SFRP1, INDO, IKBKB, POLB, VDAC3, SLC20A2, LOC114926*
9q31.3	107,000	109,000	*KLF4, EPB41L4B*
11p15.5-p15.3	400	12,022.4	*HRAS, EIF3S5, EIF4G2, IGF2, LMO1*
12p13.31	5,699	9,576.503	*VWF*
12p13.1-p12.3	12,857	15,916.1	*EPS8, RERG, ARHGDIB*
12q13.12-q14.1	46,343	58,299.56	*CDK2, CDK4, ERBB3, SAS, GLI-1, MMP19, ITGA7,GPD1*
12q14.2-q14.3	62,342	64,794.16	*HMGA2*
12q23.3	103,000	103,000	*TRA1*
12q24.23-q24.31	117,000	124,000	*EIF2B1, CDK2AP1*
12q24.33	127,000	132,000	*PXN*
13q34	110,000	114,000	*PTPN11*
14q11.2-q12	19,884	25,192.05	*DAD1, BCL2L2, RAB2B, MMP14*
14q23.2-q24.2	61,087	69,758.86	*FUT8, EIF2S1, RAB15*
14q24.3	72,262	75,186.99	*NEK9, ENTPD5, EIF2B2*
14q32.31-q32.33	98,912	105,000	*AKT1, JAG2*
15q11.2	20,524	21,438.85	*MKRN3*
15q14-q15.3	37,664	41,610.45	*RAD51*
15q21.3	50,631	52,066.41	*HNF6*
15q22.2-q22.31	58,747	66,395	*MAP2K1, MAP2K5,CA15*
15q24.3	73,972	75,550.99	*ZNF291, HMG20A*
15q26.1-q26.2	86,471	94,507.94	*NTRK3, PLIN*
17q24.3-q25.3	68,271	74,465.33	*CDC42EP4, RAB37, CDK3, SLC9A3R1*
18p11.21	10,116	13,628.32	*TNFSF5IP1*
18q21.1-q21.31	44,641	54,427.66	*WDR7, MAPK4, NEDD4L*
20p13-p12.3	151	6,720.456	*PTPRA*
21q22.11-q22.13	30,669	37,669.65	*CLDN14, RUNX1*
			Putative tumor suppressor gene
Losses			
2p12	76,415	81,844.75	*CTNNA2*
4p16.1-p15.33	7,179	15,409.73	*WDR1*
4p15.31	18,039	21,064.85	*SLIT2*
4p15.1-p14	30,425	37,344.35	*CENTD1, PCDH7*
8p23.3-p22	345	17,472.8	*DLC1, GATA4, PINX1, NEIL2, TUSC3*
10q21.1-q21.2	51,823	59,928.89	*PCDH15, DKK1*
10q23.1	82,068	85,966.8	*PCDH21*
13q12.13-q12.13	23,753	24,434.49	*PARP4*
15q12	21,482	23,337.05	*NDN, C15orf2, SNURF, UBE3A*
15q13.3-q15.1	29,169	38,061.79	*THBS1, TRPM1*
15q15.3-q21.2	41,446	48249.97	*TP53BP1*
15q21.3	50,631	55,795.41	*HNF-6*
15q24.1-q24.2	70,607	74,238.08	*NRG4, NEO1*
15q25.1-q25.2	75,852	80,209.64	*CRABP1*
18p11.31-p11.22	3,502	9,469.78	*PTPRM, DAL-1*
18q11.2-q21.1	19,363	42,965.66	*CDH2*
18q21.33-q23	59,150	72,826.14	*CDH7, CDH19*
22q11.22-q13.1	19,667	36,036.96	*CHEK2*

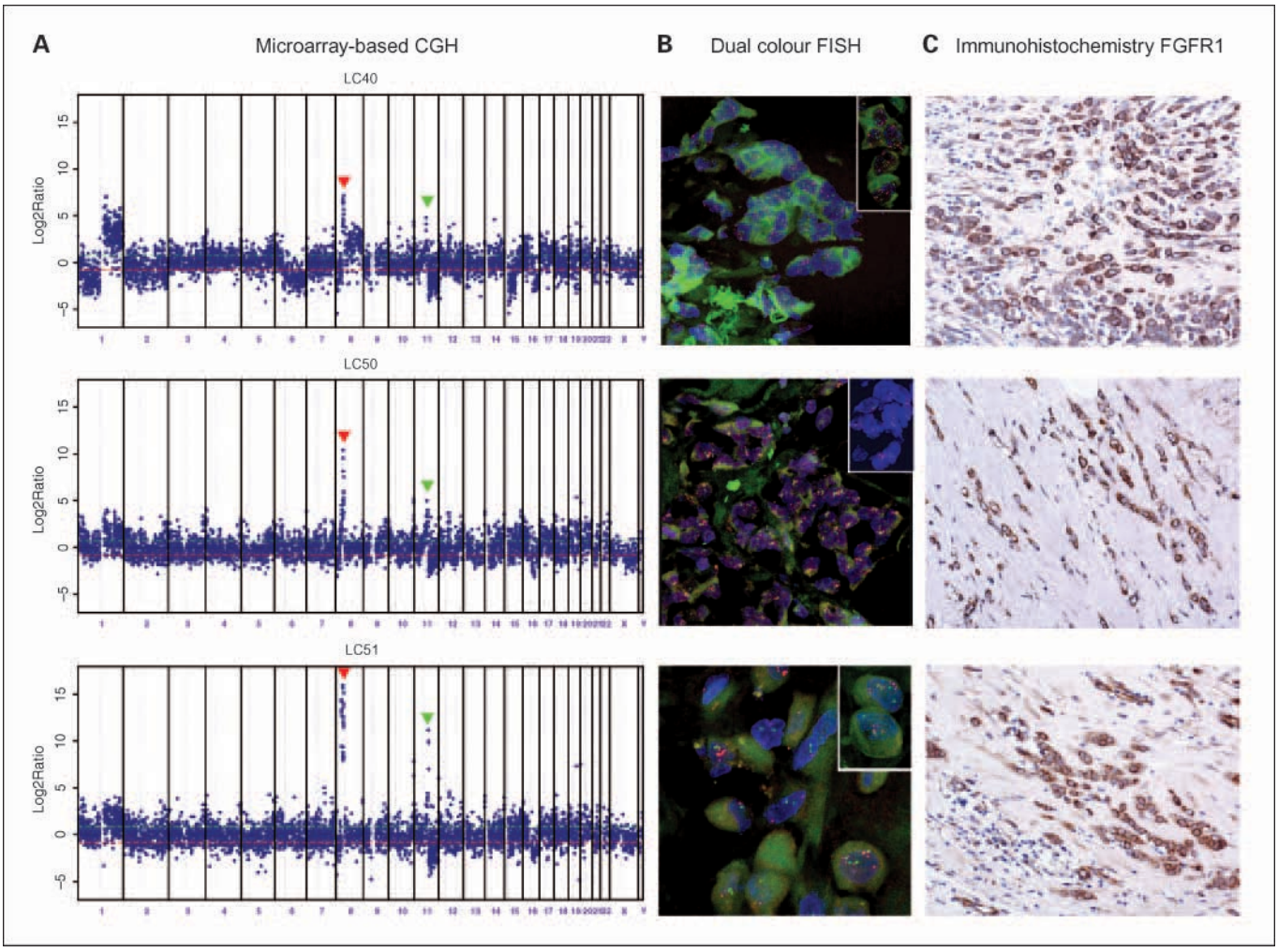

Fig. 2. CLCs with 8p12-p11.2 and 11q13 copy number gains. *A,* representative aCGH plots for three CLCs with focal copy number gain at 8p12-p11.2 (*red arrowheads*) and 11q13 (*green arrowheads*). Median absolute deviation – centered $\log_2$ ratios are plotted on the *Y*-axis against each clone according to genomic location on the *X*-axis. The centromere is represented by a vertical dotted line. Horizontal dashed lines correspond to median absolute deviation – centered $\log_2$ ratios of 0.8 and −0.8. *B,* matched representative dual-color fluorescent *in situ* hybridization for *FGFR1* (*green*) and *CCND1* (*red*). Note more than five copies of each probe/nucleus. In LC51, stromal cells showed only two copies of each probe. Inset, note the presence of more than five signals of each probe in the nuclei of neoplastic cells. *C,* immunohistochemistry for FGFR1. Note the strong membrane and cytoplasmic positivity in neoplastic cells.

Correlations between chromosomal abnormalities

Figure 1C shows the association between different gains and losses of genomic material in this series of lobular carcinomas. Despite the limited sample size, significant associations were observed. For instance, gain of 1q showed strong correlations with gain of 16p and loss of 16q. Briefly, concurrent large gains of 1q and losses of 16q were detected in 12 cases, with gains of 16p found in 8 of these 12 cases. These findings might suggest the presence of the unbalanced chromosomal translocation t(1;16)/der(1;16) (q10;p10) in these eight cases (61.5%), which is reported to be found in up to 75% of CLCs (38, 39). An association between gains of 8p12-p11.23 and 11q13.3 were also observed, which was confirmed by dual-color FISH (Fig. 2).

MDA-MB-134 as a putative model for the study of CLCs with 8p12-p11.2 and 11q13 coamplifications

To investigate whether any breast cancer cell lines had genetic changes characteristic of CLC, we examined a database of the molecular genetic profiles of 28 breast cancer cell lines generated with aCGH (40).[8] Like CLCs, the cell line MDA-MB-134 is positive for hormone receptors, lacks *HER2* amplification and overexpression, and harbored physical loss of 16q- and coamplification of 8p12-p11.21 and 11q13, and deletions of 8pter-p12 and 11q13.3-qter (refs. 28, 41–43; Fig. 3; Supplementary Table S3). Through a combination of immunohistochemistry, expression profile analysis (Supplemental Table S4), and aCGH, we confirmed previous results that this cell line expresses estrogen receptor and progesterone receptor, shows reduced levels of β-catenin, and lacks HER2 and E-cadherin expression (data not shown). In addition, the underlying genetic mechanism of CDH1 inactivation is homozygous deletion of *CDH1* gene (ref. 43; data not shown). Thus, although MDA-MB-134 is reported to be derived from an "invasive ductal carcinoma", our observations suggest that MDA-MB-134 has the hallmarks of molecular genetic and

[8] A. Mackay, manuscript in preparation.

expression profiles of CLC. The cell line ZR-75-1 also harbors loss of 16q, high-level gains on 8p12-p11.2 and 11q13.3, deletion of 11q13.3-qter, but no changes on 8p12-pter (refs. 28, 41; Fig. 3) and is positive for estrogen receptor (44). However, despite hemizygous loss of 16q, E-cadherin is expressed at normal levels (Supplementary Table S4).

FGFR1 is overexpressed when amplified in CLCs and in the MDA-MB-134 cell line

Having established the presence of an amplicon on 8p12-p11.2 in six CLCs, we sought to identify the genes showing expression changes along with copy number changes in the cell lines MDA-MB-134 and ZR-75.1. It has been shown that the amplicon on 8p12-p11 is complex in breast cancer (28, 35, 45, 46), and that it can be subdivided into four regions (28). In MDA-MB-134, two amplicons were identified: one mapping to 8p12-p11.23 spanning the region between 36.9 and 39.2 Mb and the second mapping to 8p11.21 spanning the region between 41.5 and 42.1 Mb. In ZR-75-1, the amplicon mapping to 8p12-p11.23 encompassed the region between 36.9 and 38.0 Mb, which was followed by a deletion spanning the region between 38.0 and 39.2 Mb (Fig. 3, *arrowhead*). Interestingly, this deleted region maps to *FGFR1* (Fig. 3, *arrowhead*). The deletion of the BACs encompassing this region (RP11-576M6 and RP11-551D4, Supplementary Table S3) was confirmed by FISH (data not shown). When we compared aCGH and

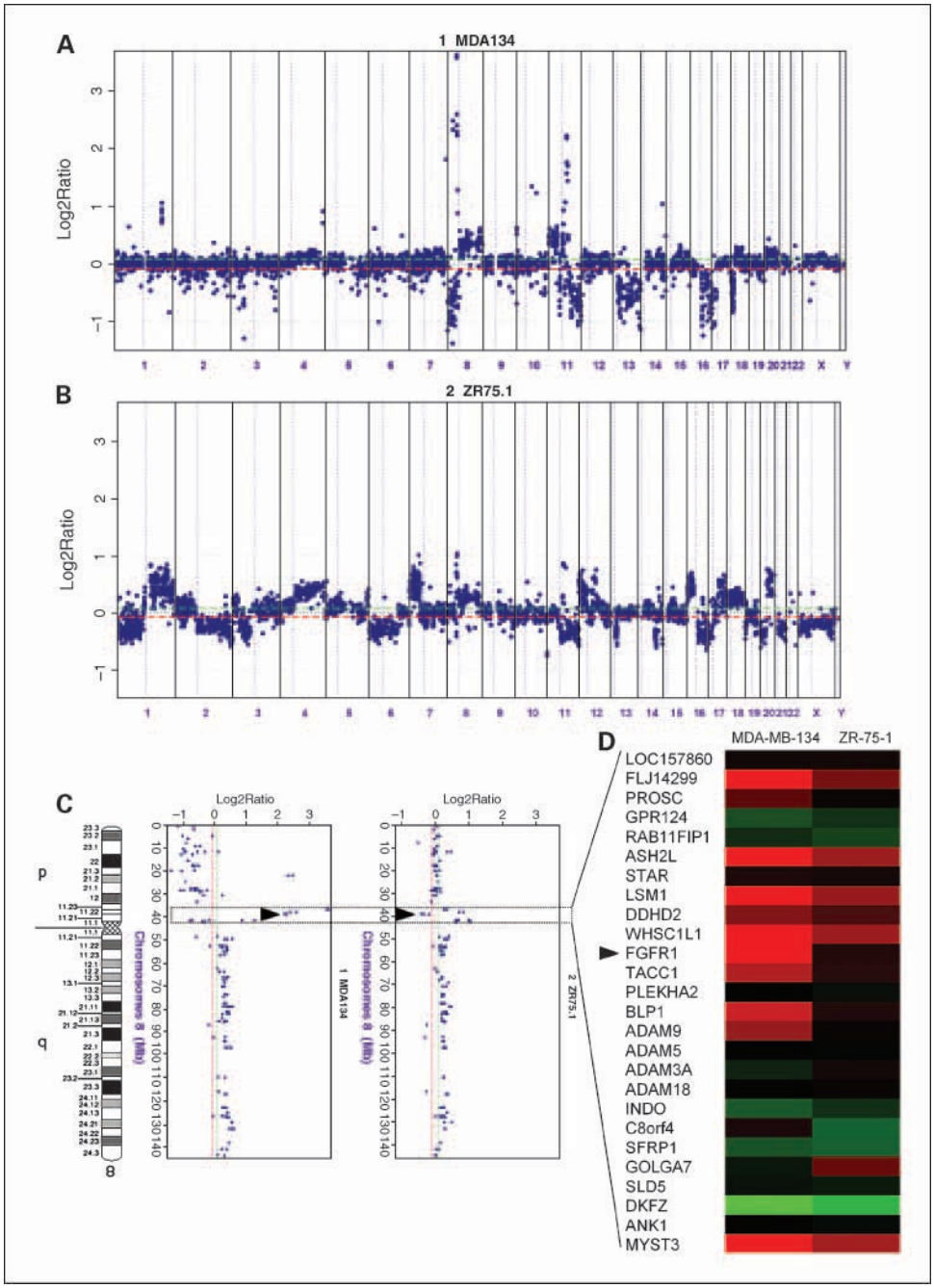

Fig. 3. MDA-MB-134 as a model for the study of CLCs with 8p12-p11.2 and 11q13 coamplifications. *A* and *B*, aCGH plots of cell lines MDA-MB-134 and ZR-75.1. Log_2 ratios are plotted on the *Y*-axis against each clone according to genomic location on the *X*-axis. Vertical dotted lines, the centromeres; horizontal dashed lines, log_2 ratios of 0.8 and −0.8. Note that both cell lines harbor high-level gains of 8p11.2-p12 and 11q13. *C,* detailed view of the amplicon on 8p11.2-8p12 (*dashed-line box*). Note that clones mapping to *FGFR1* are amplified in MDA-MB-134, whereas the ZR-75.1 cell line harbors a microdeletion in this genomic region. *D,* heat map of the expression levels of genes mapping to the amplicon on 8p11.2-p12 in MDA-MB-134 and ZR-75-1 cell lines. Colors represent relative levels of gene expression: high levels of expression (*brightest red*) and low levels or absence of expression (*green*) when compared with universal human reference RNA.

expression profiling data in these two cell lines, the *FGFR1* gene was highly expressed in MDA-MB-134, whereas it showed low expression levels in ZR-75-1 (Fig. 3). Other genes that were both amplified and up-regulated in both cell lines included *FLJ14299*, *PROSC*, *RAB11FIP1*, *ASH2L*, *WHSC1L1*, *BLP1*, and *MYST3* (Fig. 3). When samples of CLC were subjected to immunohistochemical analysis, all cases (n = 6) with *FGFR1* copy number gains also showed protein overexpression (Fig. 2). Taken together, these data are consistent with the notion that when *FGFR1* is amplified, it is also overexpressed.

FGFR1 contributes to the survival of MDA-MB-134 cells

To determine whether *FGFR1* is a potential driver of the 8p12 amplicon and contributes to the survival of MDA-MB-134 cells, we transfected MDA-MB-134 cells with siRNA directed against *FGFR1* or nontargeting control siRNA (Scram). Transfection of MDA-MB-134 cells with *FGFR1* siRNA reduced cell viability in comparison to Scram control (Fig. 4), suggesting that *FGFR1* is required for the survival of MDA-MB-134 cells. In addition, when ZR-75-1 cells were transfected with siRNA directed against *FGFR1* and nontargeting controls, no statistically significant differences in cell viability were detected (data not shown).

To further examine the importance of *FGFR1* in the survival of MDA-MB-134, we used a specific *FGFR1* tyrosine kinase inhibitor, SU5402. MDA-MB-134 cells, and for comparison, breast cancer cell lines, ZR-75-1, MCF7, and CAL51, which show no *FGFR1* gene copy number gains (data not shown), were treated with a range of concentrations of SU5042 and assessed for survival. MDA-MB-134 cells were significantly more sensitive to SU5402 than all other cell lines lacking *FGFR1* amplification (P = 0.0237, ANOVA test; 10^{-5} mol/L SU5402; Fig. 4). This supports the siRNA experiments and further implicates *FGFR1* signaling in the survival of MDA134 cells.

Discussion

The molecular genetic features of lobular breast carcinomas have received great attention in the literature in the last few years (1, 2, 5–7, 9–13, 21). Inactivation of the *CDH1* gene through physical loss of 16q associated with *CDH1* gene mutation and/or promoter methylation leads to the abrogation of E-cadherin expression. Together with gains of 1q, these are currently accepted hallmark molecular features of *in situ* and invasive lobular carcinomas (1–3, 5–7, 9–13, 21). However, little is known about other genetic changes driving the pathogenesis of CLCs. The present study not only confirms the known molecular genetic features of CLCs (1–3, 5–7, 9–13, 21), but also shows that CLCs harbor a greater genetic complexity and a higher number of recurrent genomic changes than previously appreciated with other molecular techniques (12, 13). In fact, recurrent gains on 1q, 5p, 7q, 11p, 11q, 12q, 14q, 16p, 18p, 19p+q, and 20p+q and losses on chromosomes 11q, 13q, 16q, 18q, and Xq were observed in >30% of the CLCs analyzed.

Complex genomic changes involving 11q were identified. Gains of 11q13 specifically mapping to *CCND1* were observed in 53% of all CLCs. *CCND1* copy number gains and *CCND1* overexpression have been reported to be a feature of low grade, estrogen receptor–positive tumors (16, 17, 34, 47), including CLCs (12, 13, 16, 17). In addition, losses of 11q14.1-q25 were observed in 53.8% of the cases. Although these gains and deletions have not been reported in chromosomal CGH analyses of CLCs, Loo et al. (12) and Shelley-Hwang et al. (13) showed frequent recurrent gains of 11q13 followed by genomic losses in more telomeric regions of 11q in CLCs.

There is compelling evidence to suggest that DNA amplification at 8p12-p11.2 has a remarkably complex structure (28), encompassing at least four distinct amplification cores. In the present study, *FGFR1* was amplified in all lobular carcinomas harboring the 8p12-p11.2 amplicon, suggesting that tumors of different types or grades may have specific, and distinct, amplicon drivers within the 8p locus (16, 26, 34, 35, 45). Alternatively, this may indicate that tumors of different histologic grades or histologies may acquire distinct genetic changes through different molecular mechanisms (1–3). Although *FGFR1* may not be the sole oncogene in

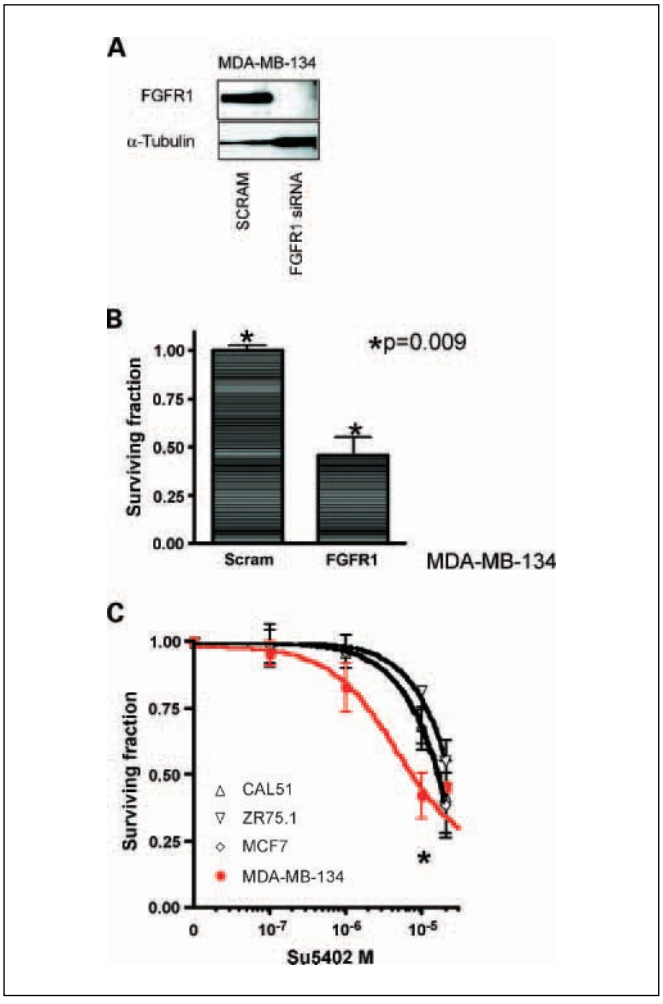

Fig. 4. Effect of FGFR1 inhibition in MDA-MB-134 cells. *A,* Western blot analysis of MDA-MB-134 cells after transfection with siRNA directed against FGFR1 or nontargeting control siRNA (Scram). *B,* transfection of MDA-MB-134 cells with *FGFR1* siRNA reduced cell viability in comparison with Scram controls. *C,* MDA-MB-134, ZR-75-1, MCF7, and CAL51 cell lines were treated with a specific FGFR1 tyrosine kinase inhibitor, SU5402, and anchorage-dependent survival was assessed. Note that MDA-MB-134 cells were more sensitive to SU5402 than all other cell lines lacking *FGFR1* amplification and overexpression. *, P = 0.237 (ANOVA). The IC_{50} values for each cell line were, as follows: MDA-MB-134, 7 μmol/L; ZR-75-1, >20 μmol/L; MCF7; 16 μmol/L; and CAL51, 17 μmol/L.

the 8p12-p11.2 amplification observed in breast carcinomas (26, 28, 29, 35, 45, 46), in the present study, we show that this oncogene was concurrently amplified and overexpressed in 43% of CLCs. Furthermore, *FGFR1* expression and activation were required for the survival of MDA-MB-134 cells. Given the striking similarities between grade 1 and 2 CLCs, and grade 1 ductal carcinomas at the genetic level (1–3), further studies are required to determine whether this genetic subgroup of breast carcinomas harboring 1q+, 16q−, and *FGFR1* and 11q13 amplifications are characterized by a lobular phenotype or if this is a more pervasive genotype within the group of low grade breast carcinomas. In fact, there are several lines of evidence to suggest that FGFR1 may play an important role in the biology of estrogen receptor–positive breast carcinomas of both lobular and low grade ductal histologies (16, 34). In a recent study, Xian et al. (48) introduced a drug-inducible *FGFR1* gene into HC11 mouse mammary epithelial cells and found that *FGFR1* expression led to the reinitiation of cell proliferation, increased survival of luminal cells, and loss of cell polarity. Interestingly, *FGFR1* activation induced the up-regulation of matrix metalloproteinase 3, which in turn, caused the cleavage of E-cadherin (48). Therefore, *FGFR1* amplification and overexpression may constitute an additional mechanism for E-cadherin down-regulation in CLCs.

The present study also emphasizes the importance of fine mapping of amplicons and that amplicons like 8p12-p11.2 are likely to have different amplicon drivers in different settings. In studies in which amplifications mapping to 8p12-p11.2 were treated as a single amplicon (45, 49), *FGFR1* was ruled out as a possible amplicon driver (45, 49). However, neither the cell lines studied by Ray et al., which lacked *FGFR1* expression, harbored *FGFR1* amplification (49, 50), nor did the minimally amplified region defined by Garcia et al. (45) encompass *FGFR1*. On the other hand, there are several lines of evidence, including the data presented here, to suggest that this tyrosine kinase receptor is amplified and overexpressed in breast cancers and breast cancer cell lines (28, 32). Our results on the correlations between gene copy numbers and expression level for MDA-MB-134 and ZR-75-1 provide further evidence for this concept: although both cell lines show gain at 8p12-p11.2, the former harbors *FGFR1* amplification and overexpression, whereas the latter does not.

In conclusion, this study shows that CLCs harbor more molecular genetic changes than previously appreciated and provides comprehensive lists of putative oncogenes and tumor suppressor genes frequently altered in CLCs. Apart from recurrent gains of 1q and physical losses of 16q, a subset of CLCs harbors concurrent gains of 8p12-p11 and 11q13. Furthermore, we have identified a frequent amplification/overexpression of *FGFR1* in this subset of CLCs, suggesting that small molecules or antibodies directed against FGFR1 should be investigated as novel therapeutic strategies against this tumor type. Finally, MDA-MB-134 cells may provide a useful model system for the necessary mechanistic and preclinical investigations of breast carcinomas with *FGFR1* amplification and overexpression.

References

1. Simpson PT, Reis-Filho JS, Gale T, Lakhani SR. Molecular evolution of breast cancer. J Pathol 2005;205:248–54.
2. Reis Filho JS, Simpson PT, Gale T, Lakhani SR. The molecular genetics of breast cancer: the contribution of comparative genomic hybridization. Pathol Res Pract 2005;201:713–25.
3. Stange DE, Radlwimmer B, Schubert F, et al. High-resolution genomic profiling reveals association of chromosomal aberrations on 1q and 16p with histologic and genetic subgroups of invasive breast cancer. Clin Cancer Res 2006;12:345–52.
4. Rakha EA, Green AR, Powe DG, Roylance R, Ellis IO. Chromosome 16 tumor-suppressor genes in breast cancer. Genes Chromosomes Cancer 2006;45:527–35.
5. Berx G, Cleton-Jansen AM, Nollet F, et al. E-cadherin is a tumour/invasion suppressor gene mutated in human lobular breast cancers. EMBO J 1995;14:6107–15.
6. Sarrio D, Moreno-Bueno G, Hardisson D, et al. Epigenetic and genetic alterations of APC and CDH1 genes in lobular breast cancer: relationships with abnormal E-cadherin and catenin expression and microsatellite instability. Int J Cancer 2003;106:208–15.
7. Droufakou S, Deshmane V, Roylance R, Hanby A, Tomlinson I, Hart IR. Multiple ways of silencing E-cadherin gene expression in lobular carcinoma of the breast. Int J Cancer 2001;92:404–8.
8. Brooks-Wilson AR, Kaurah P, Suriano G, et al. Germline E-cadherin mutations in hereditary diffuse gastric cancer: assessment of 42 new families and review of genetic screening criteria. J Med Genet 2004;41:508–17.
9. Etzell JE, Devries S, Chew K, et al. Loss of chromosome 16q in lobular carcinoma *in situ*. Hum Pathol 2001;32:292–6.
10. Nishizaki T, Chew K, Chu L, et al. Genetic alterations in lobular breast cancer by comparative genomic hybridization. Int J Cancer 1997;74:513–7.
11. Lu YJ, Osin P, Lakhani SR, Di Palma S, Gusterson BA, Shipley JM. Comparative genomic hybridization analysis of lobular carcinoma *in situ* and atypical lobular hyperplasia and potential roles for gains and losses of genetic material in breast neoplasia. Cancer Res 1998;58:4721–7.
12. Loo LW, Grove DI, Williams EM, et al. Array comparative genomic hybridization analysis of genomic alterations in breast cancer subtypes. Cancer Res 2004;64:8541–9.
13. Shelley-Hwang E, Nyante SJ, Yi Chen Y, et al. Clonality of lobular carcinoma *in situ* and synchronous invasive lobular carcinoma. Cancer 2004;100:2562–72.
14. Hoff ER, Tubbs RR, Myles JL, Procop GW. HER2/neu amplification in breast cancer: stratification by tumor type and grade. Am J Clin Pathol 2002;117:916–21.
15. Arpino G, Bardou VJ, Clark GM, Elledge RM. Infiltrating lobular carcinoma of the breast: tumor characteristics and clinical outcome. Breast Cancer Res 2004;6:R149–56.
16. Courjal F, Cuny M, Simony-Lafontaine J, et al. Mapping of DNA amplifications at 15 chromosomal localizations in 1875 breast tumors: definition of phenotypic groups. Cancer Res 1997;57:4360–7.
17. Oyama T, Kashiwabara K, Yoshimoto K, Arnold A, Koerner F. Frequent overexpression of the cyclin D1 oncogene in invasive lobular carcinoma of the breast. Cancer Res 1998;58:2876–80.
18. Smith DB, Howell A, Wagstaff J. Infiltrating lobular carcinoma of the breast: response to endocrine therapy and survival. Eur J Cancer Clin Oncol 1987;23:979–82.
19. Cocquyt VF, Blondeel PN, Depypere HT, et al. Different responses to preoperative chemotherapy for invasive lobular and invasive ductal breast carcinoma. Eur J Surg Oncol 2003;29:361–7.
20. Cristofanilli M, Gonzalez-Angulo A, Sneige N, et al. Invasive lobular carcinoma classic type: response to primary chemotherapy and survival outcomes. J Clin Oncol 2005;23:41–8.
21. Reis-Filho JS, Simpson PT, Jones C, et al. Pleomorphic lobular carcinoma of the breast: role of comprehensive molecular pathology in characterization of an entity. J Pathol 2005;207:1–13.
22. Lambros MBK, Simpson PT, Jones C, et al. Unlocking pathology archives for molecular genetic studies: a reliable method to generate probes for chromogenic and fluorescent *in situ* hybridisation. Lab Invest 2006;86:398–408.
23. Mohammadi M, McMahon G, Sun L, et al. Structures of the tyrosine kinase domain of fibroblast growth factor receptor in complex with inhibitors. Science 1997;276:955–60.
24. Iafrate AJ, Feuk L, Rivera MN, et al. Detection of large-scale variation in the human genome. Nat Genet 2004;36:949–51.
25. Sharp AJ, Locke DP, McGrath SD, et al. Segmental duplications and copy-number variation in the human genome. Am J Hum Genet 2005;77:78–88.
26. Pole JC, Courtay-Cahen C, Garcia MJ, et al. High-resolution analysis of chromosome rearrangements on 8p in breast, colon and pancreatic cancer reveals a complex pattern of loss, gain and translocation. Oncogene 2006: Epub ahead of print [doi: 10.1038/sj.onc.1209570].
27. Coquelle A, Pipiras E, Toledo F, Buttin G, Debatisse M. Expression of fragile sites triggers intrachromosomal mammalian gene amplification and sets boundaries to early amplicons. Cell 1997;89:215–25.
28. Gelsi-Boyer V, Orsetti B, Cervera N, et al. Comprehensive profiling of 8p11–12 amplification in breast cancer. Mol Cancer Res 2005;3:655–67.
29. Adelaide J, Huang HE, Murati A, et al. A recurrent chromosome translocation breakpoint in breast and pancreatic cancer cell lines targets the neuregulin/

NRG1 gene. Genes Chromosomes Cancer 2003;37:333–45.

30. Dib A, Adelaide J, Chaffanet M, et al. Characterization of the region of the short arm of chromosome 8 amplified in breast carcinoma. Oncogene 1995;10:995–1001.

31. Luqmani YA, Graham M, Coombes RC. Expression of basic fibroblast growth factor, FGFR1 and FGFR2 in normal and malignant human breast, and comparison with other normal tissues. Br J Cancer 1992;66:273–80.

32. Jacquemier J, Adelaide J, Parc P, et al. Expression of the FGFR1 gene in human breast-carcinoma cells. Int J Cancer 1994;59:373–8.

33. Ugolini F, Adelaide J, Charafe-Jauffret E, et al. Differential expression assay of chromosome arm 8p genes identifies Frizzled-related (FRP1/FRZB) and Fibroblast Growth Factor Receptor 1 (FGFR1) as candidate breast cancer genes. Oncogene 1999;18:1903–10.

34. Cuny M, Kramar A, Courjal F, et al. Relating genotype and phenotype in breast cancer: an analysis of the prognostic significance of amplification at eight different genes or loci and of p53 mutations. Cancer Res 2000;60:1077–83.

35. Prentice LM, Shadeo A, Lestou VS, et al. NRG1 gene rearrangements in clinical breast cancer: identification of an adjacent novel amplicon associated with poor prognosis. Oncogene 2005;24:7281–9.

36. Still IH, Hamilton M, Vince P, Wolfman A, Cowell JK. Cloning of TACC1, an embryonically expressed, potentially transforming coiled coil containing gene, from the 8p11 breast cancer amplicon. Oncogene 1999;18:4032–8.

37. Cleator S, Tsimelzon A, Ashworth A, et al. Gene expression patterns for doxorubicin (Adriamycin) and cyclophosphamide (Cytoxan) (AC) response and resistance. Breast Cancer Res Treat 2005;37:1–5.

38. Tsuda H, Takarabe T, Hirohashi S. Correlation of numerical and structural status of chromosome 16 with histological type and grade of non-invasive and invasive breast carcinomas. Int J Cancer 1999;84:381–7.

39. Flagiello D, Gerbault-Seureau M, Sastre-Garau X, Padoy E, Vielh P, Dutrillaux B. Highly recurrent der(1;16)(q10;p10) and other 16q arm alterations in lobular breast cancer. Genes Chromosomes Cancer 1998;23:300–6.

40. Iravani M, Fenwick K, Grigoriadis A, et al. Integrated molecular profiling of human breast cell types and breast cancer cell lines using expression microarrays and array CGH [abstract]. Breast Cancer Res Treat 2005;94:S27.

41. Davidson JM, Gorringe KL, Chin SF, et al. Molecular cytogenetic analysis of breast cancer cell lines. Br J Cancer 2000;83:1309–17.

42. Bautista S, Theillet C. CCND1 and FGFR1 coamplification results in the colocalization of 11q13 and 8p12 sequences in breast tumor nuclei. Genes Chromosomes Cancer 1998;22:268–77.

43. Hiraguri S, Godfrey T, Nakamura H, et al. Mechanisms of inactivation of E-cadherin in breast cancer cell lines. Cancer Res 1998;58:1972–7.

44. Warri AM, Laine AM, Majasuo KE, Alitalo KK, Harkonen PL. Estrogen suppression of erbB2 expression is associated with increased growth rate of ZR-75-1 human breast cancer cells *in vitro* and in nude mice. Int J Cancer 1991;49:616–23.

45. Garcia MJ, Pole JC, Chin SF, et al. A 1 Mb minimal amplicon at 8p11–12 in breast cancer identifies new candidate oncogenes. Oncogene 2005;24:5235–45.

46. Huang HE, Chin SF, Ginestier C, et al. A recurrent chromosome breakpoint in breast cancer at the NRG1/neuregulin 1/heregulin gene. Cancer Res 2004;64:6840–4.

47. Al-Kuraya K, Schraml P, Torhorst J, et al. Prognostic relevance of gene amplifications and coamplifications in breast cancer. Cancer Res 2004;64:8534–40.

48. Xian W, Schwertfeger KL, Vargo-Gogola T, Rosen JM. Pleiotropic effects of FGFR1 on cell proliferation, survival, and migration in a 3D mammary epithelial cell model. J Cell Biol 2005;171:663–73.

49. Ray ME, Yang ZQ, Albertson D, et al. Genomic and expression analysis of the 8p11–12 amplicon in human breast cancer cell lines. Cancer Res 2004;64:40–7.

50. Yang ZQ, Albertson D, Ethier SP. Genomic organization of the 8p11–12 amplicon in three breast cancer cell lines. Cancer Genet Cytogenet 2004;155:57–62.